2-2017

Effects of Microstructure on the Strain Rate Sensitivity of Advanced Steels

Rakan Alturk
Clemson University, ralturk@clemson.edu

Steven Mates
National Institute for Standards and Technology

Zeren Xu
Clemson University

Fadi Abu-Farha
Clemson University

Effects of Microstructure on the Strain Rate Sensitivity of Advanced Steels

Rakan Alturk[1], Steven Mates[2], Zeren Xu[1], Fadi Abu-Farha[1*]

[1]Clemson University – International Center for Automotive Research (CU-ICAR), Greenville, SC, USA
[2]National Institute for Standards and Technology, Gaithersburg, MD, USA

[*] Corresponding Author. Tel.: +1 864 283 7231; E-mail: FADI@clemson.edu

Abstract

The dependence of the strain rate sensitivity of advanced ~1GPa tensile strength steels on the phases present in their microstructures was studied by testing different steels at 0.005 s^{-1} and 500 s^{-1}. The high strain rate tests were performed using a Kolsky bar setup, while the quasi-static tests were performed using a universal testing machine. The two main steels of interest were the Ferrite-Martensite DP980 and the Ferrite-Martensite-Austenite QP980; the latter being a transformation induced plasticity (TRIP) assisted steel. For comparison, ferritic CR5 mild steel and austenitic stainless steel 201 were also tested under the same conditions. Though the differences in the steel chemistries were not taken into account, the results obtained here suggest a strong relationship between the phase-content of the steel and its response to the changes in the loading rate. The relationships between the observed mechanical behavior and the phases present in the microstructure are discussed.

Keywords: High Rate Deformation, Microstructure, AHSSs, Kolsky Bar, Rate Sensitivity

1 Introduction

With the ever-increasing push for lightweighting in the automotive sector, Advanced High Strength Steels (AHSSs) continue to infiltrate the industry due to their unique properties and merits [1]. The uniqueness of AHSSs can be primarily attributed to their complex multi-phase microstructures, as compared to conventional single-phase steels, which enable achieving particular blends of strength and ductility. While strength drives the lightweighting potential of the material, ductility defines the practical limits of its stamping. However, beyond forming materials into the various automotive components, materials need to pass specific tests and meet certain criteria to be used in vehicles; some of the most critical ones are crashworthiness-related [2]. Finite element (FE) analyses are typically performed to simulate a crash event; the accuracy of these simulations rely heavily on how well the constitutive equations describe the material behavior.

Automotive materials undergo loading at different strain rates during their lifetime. From quasi-static (< 0.1 s^{-1}) to intermediate (around 1 s^{-1}) during stamping, to high rates (>100 s^{-1}) during a crash event. It is well-established in the literature that the deformation behavior and the properties of steels are highly influenced by strain rate. Thus, the governing equations used in the various analyses should be able to incorporate rate effects on the behavior of the material.

Strain rate effects on the mechanical properties of steels have been studied by many researchers over the past decade; examples include these references [3-17]. However, the majority of these studies did not focus on the microstructure and the role it plays in dictating the strain rate sensitivity of the steel grade [3-14]. Few studies considered the microstructure and its correlation to rate sensitivity, particularly in advanced steel grades. Hwang et. al [15] studied the effects of ferrite grain size on the strain rate sensitivity in DP steels. Oliver et. al [16] tested DP and TRIP steels at 0.001 s^{-1} and 200 s^{-1} to compare the changes in the microstructure at different strain rates. Tarigopula et. al [3] studied the effect of strain rate on the mechanical properties and strain localization of DP800. Li et. al [17] studied the effects of strain rate on deformation-induced transformation of austenite in quenched and partitioned steels, up to strain rates of 0.1s^{-1}.

This work investigates the response of selected advanced steels with complex multiphase microstructures to external loading at rates close to those encountered during a crash event. The response is compared to that at quasi-static rates to evaluate the rate sensitivity of each material. Moreover, the differences in their responses are correlated to the types of constituent phases present in their microstructures. This would be the first step to develop models that can incorporate rate effects in each of the various phases within the microstructure of advanced high strength steels. The main two materials of interest in this study are ~1GPa tensile strength steel grades: DP980 and QP980. Nevertheless, the deformation of two single-phase steels, ferritic CR5 mild steel and austenitic stainless steel 201, are also investigated to provide some basis for comparison, and establish the rate dependency of the individual phases.

2 Experiments

2.1 Materials and Initial Microstructures

The initial microstructures of the four materials were examined by optical microscopy and scanning electron microscopy; the obtained micrographs are shown in Figure 1. The CR5, a very ductile grade of mild steel, shows a typical ferrite microstructure with a heterogeneous distribution of small and large grains (~5-25 µm equivalent grain size). The SS 201 is an austenitic stainless steel, the microstructure of which exhibits similar heterogeneous distribution of grains, though larger than the CR5. The micrograph of DP980, a dual phase steel, clearly shows the distinction between ferrite (light) and martensite (dark) in the microstructure. The area fractions of the two phases (both are very fine) were measured to be ~30% ferrite and ~70% martensite. The QP980, on the other hand, is mainly composed of ~40% ferrite, ~50% martensite and ~10% retained austenite. The ferrite and martensite grains are fine (similar to the DP980), while the austenite islands are particularly small (~0.5-1 µm); an example is indicated in the micrograph in Figure 1d. As noted, phase distinction in this material is very difficult; thus the reported phase fractions were obtained from both optical microscopy and EBSD maps (not presented here).

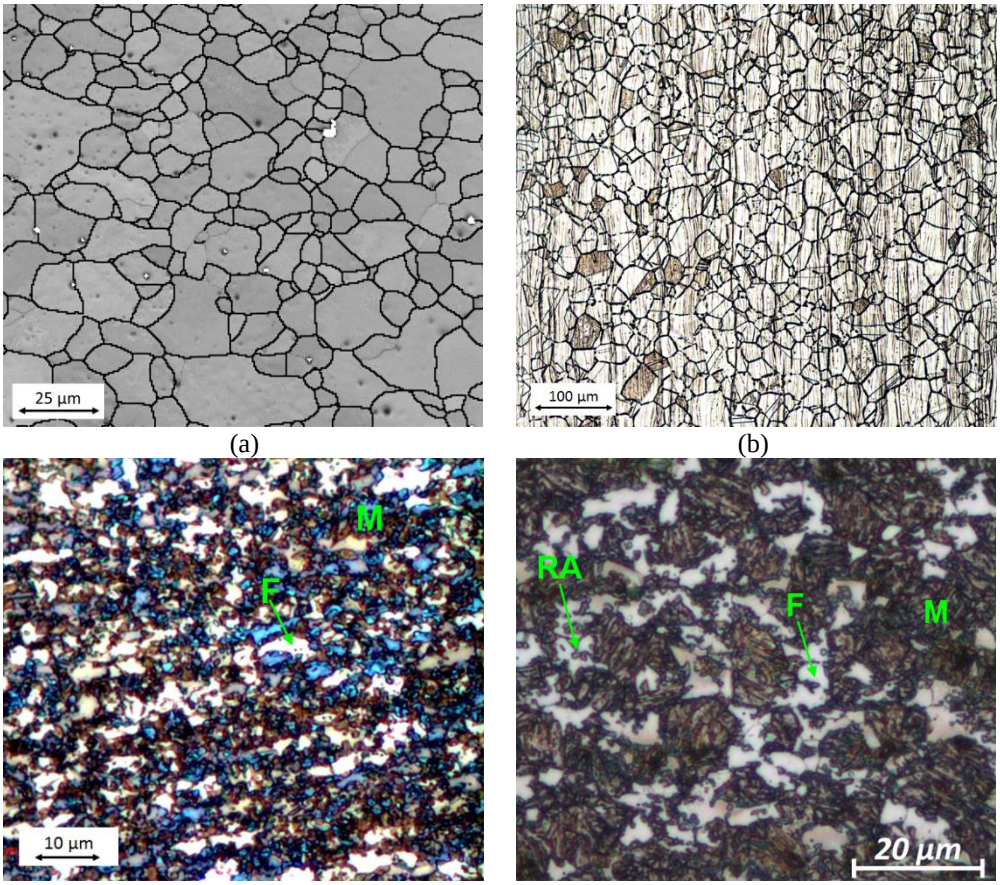

Figure 1: Micrographs showing the microstructure of the as-received material for (a) CR5 (b) SS 201 (c) DP980 and (d) QP980.

2.2 Experimental Setups and Procedure

The four materials were tested in tension under both quasi-static and high rate conditions using the setups shown in Figure 2. The quasi-static tension tests were performed on a universal electromechanical load frame, at a constant crosshead speed of 18mm/min. A standard ASTM E8 specimen geometry was used, and the corresponding strain rate of deformation was ~0.005 s^{-1}. For accurate strain measurements, a 3D digital image correlation (DIC) system was used to monitor material deformation during testing. High strain rate testing, on the other hand, was performed at the

National Institute for Standards and Technology (NIST) using the Kolsky bar setup shown in Figure 2b. Details on the testing can be found elsewhere [18]. For force measurements, 1000Ω strain gauges were bonded to the transmission bar. For strain measurements, two DIC high speed cameras were used to capture images of the specimens during testing at a frame rate of 75000 frames/s, at a resolution of 192 x 336 pixels. The actual strain rate obtained during Kolsky bar testing depends on the pressure, the incident bar length and the specimen geometry. Testing reported in this work was carried out at a particular set of conditions to achieve the desired strain rate; the pressure was set to ~30 psi, the incident bar length was chosen to be 1m, and with a 10mm gage length specimen, a strain rate of ~500 s^{-1} was achieved (measured by DIC). After testing, all DIC images, for both quasi-static and high rate testing, were processed in a consistent fashion using the same commercial DIC software to obtain the full-field history of strains during testing.

All test specimens were prepared by waterjet cutting to obtain a good edge quality. While quasi-static testing is standardized (following the ASTM-E8), there is no clear standard for the specimen geometry to be used at high rates in Kolsky bar testing. Also, it is challenging to achieve stress equilibrium in the gauge area while keeping a uniaxial stress state as there is a tradeoff between stress uniformity and the desired maximum strain rate that is also influenced by the strain hardening behavior of the material. The geometry used here is based on previous optimization that was done in a separate study.

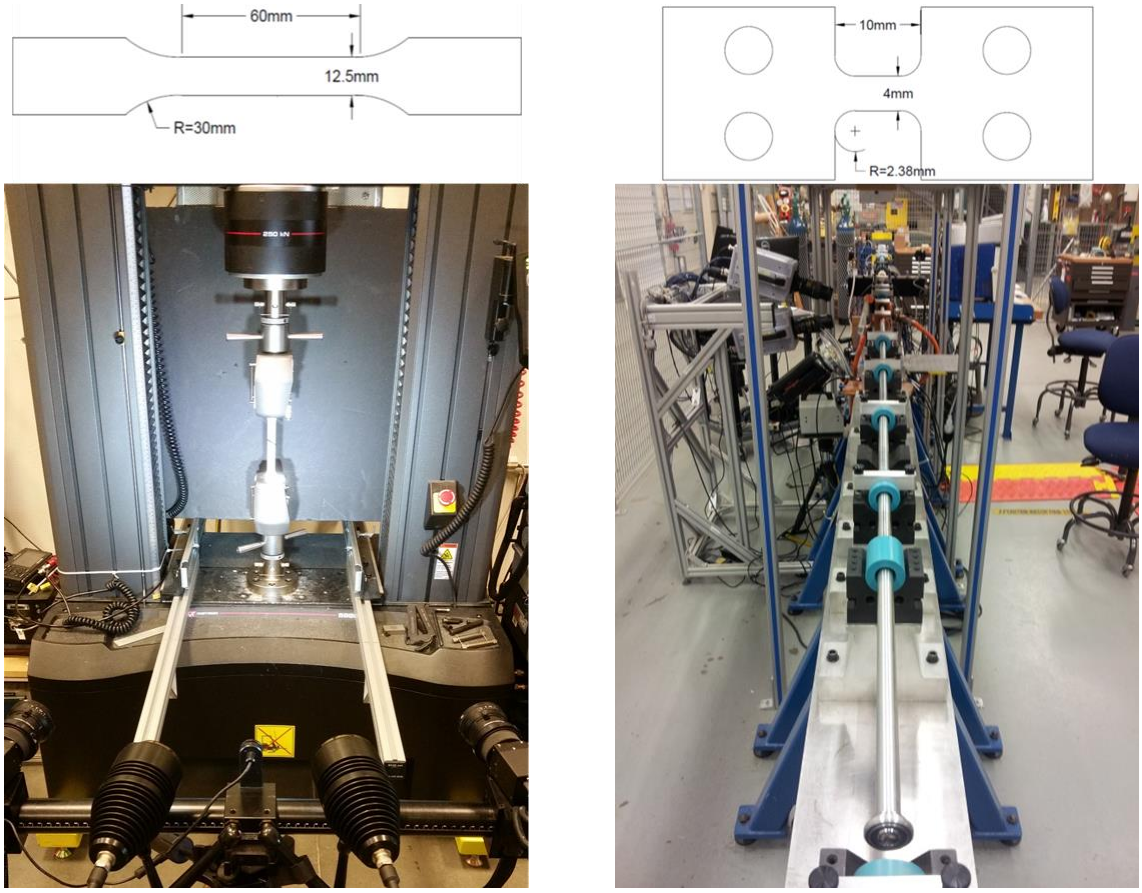

(a) (b)

Figure 2: Experimental setups and test specimens used for (a) quasi-static testing and (b) high rate testing (Kolsky)

3 Results

3.1 Flow Behavior

Engineering stress-strain curves obtained at low and high strain rates are shown for all four materials in Figure 3. Part (a) shows the clear distinction in behavior for CR5 at 0.005 s^{-1} and 500 s^{-1}. A significant increase in the yield strength and the ultimate strength is noted for the higher strain rate, accompanied by a reduction in the uniform and total elongation of the material; this is indicative of strong strain rate sensitivity. The shape of the stress-strain curve

is also different at high strain rate; the material exhibits lower strain hardening at 500 s^{-1}. This is a typical behavior of mild steels and several researchers have reported the same behavior in previous studies [7, 11, 19]. Positive strain rate sensitivity is also observed in the austenitic stainless steel 201, with a significant increase in the yield strength. Important to note here is that, for the SS 201, fracture could not be achieved after the first pulse during Kolsky bar testing (due to the extreme ductility of the material), so the dynamic stress/strain curve shown in Figure 3b is incomplete. It is therefore not possible to make a clear conclusion in regards to the tensile strength, uniform and total elongation of the material at ~500 s^{-1}. Nevertheless, testing was performed on this material in another study using a high speed servo-hydraulic machine, the results of which are included in Figure 3b. The plot shows an increase in yield strength, a slight increase in the tensile strength and a drop in the uniform ductility; total elongation is similar to that at quasi-static conditions.

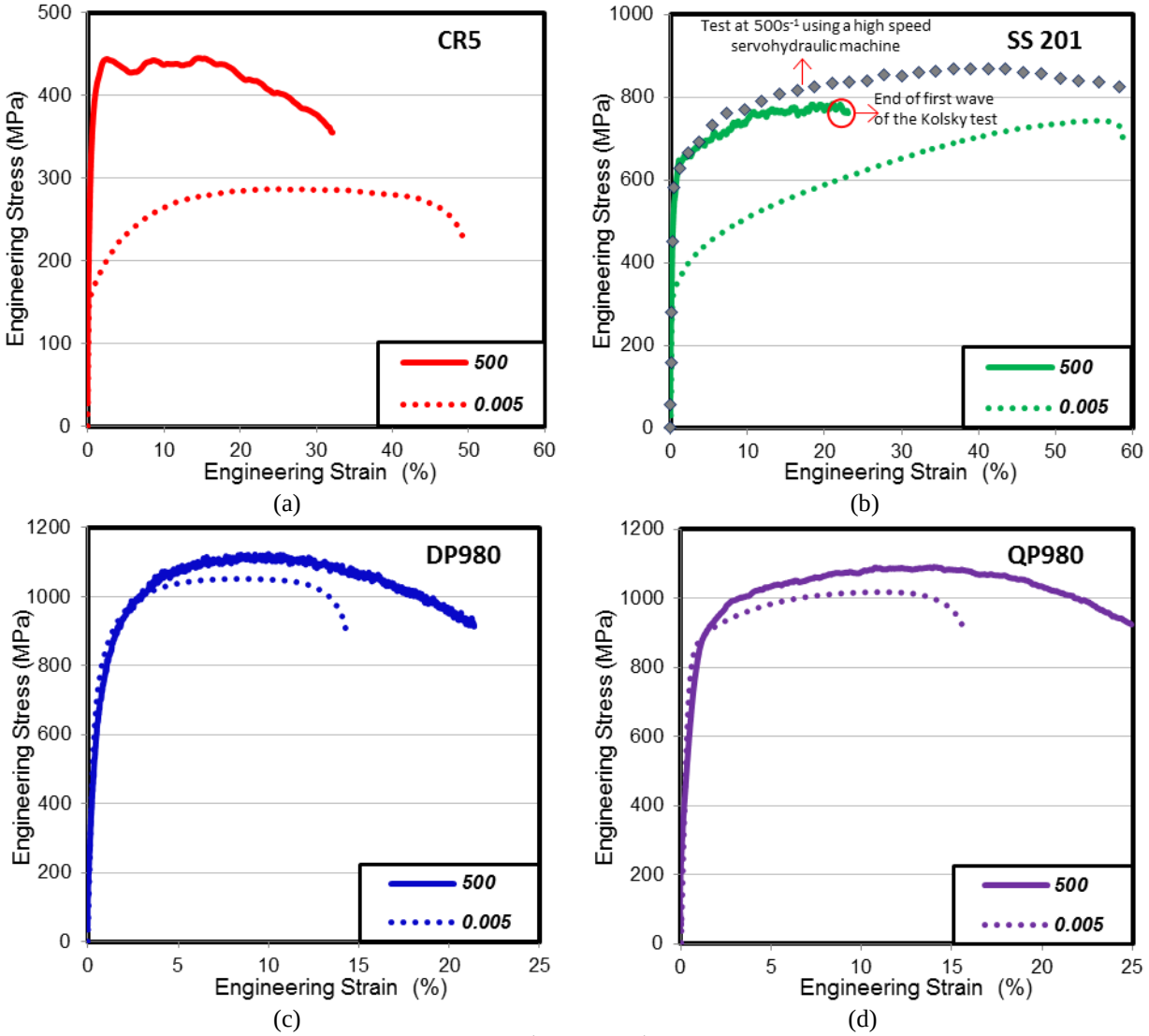

Figure 3: Engineering stress/strain curves at 0.005s^{-1} and 500s^{-1} for (a) CR5 (b) SS 201 (c) DP980 and (d) QP980.

A different behavior is observed in the multiphase steels; the DP980 and QP980 (Figure 3c and d); overall, there is a small difference between the quasi-static results and the high strain rate results. The yield and ultimate strengths change slightly with the increase in strain rate. Total elongation is notably larger at high rate in both cases; the change in the uniform elongation, however, is not as notable, and stays almost the same for the DP980. The stress/strain curves do not show the change in shape observed in CR5 and SS 201; i.e., significant drop in strain hardenability at higher rates. On the contrary, the DP980 in particular seems to strain harden more during high rate deformation, while QP980 does not show any notable change between the two rates.

3.2 Strain Rate Sensitivity

To take a closer quantitative look at the strain rate sensitivity, the percentage change in four mechanical properties between 0.005 s^{-1} and 500 s^{-1} was calculated and plotted in Figure 4. Part (a) shows how strain rate affects the yield strength in the four materials. As expected, the largest increase in the yield strength was observed in CR5, which showed an increase of ~105%, followed by SS 201, which showed an increase of ~79%. On the other hand, the yield strength of DP980 and QP980 only increased by ~2% and ~9%, respectively. The same trend was observed when comparing the change of ultimate tensile strength in Figure 4b, but the values were different. The difference in the values is due to the difference in the strain hardening behavior of the materials at high rates. As observed in the stress strain curves of CR5, the material doesn't show any significant hardening behavior in the high rate regime. While for SS 201, the material does harden at high rates but significantly less than in the quasi-static rate regime. As a result, the percentage increase in ultimate tensile strength for CR5 was ~57%, and that of SS 201 was ~21%. For DP980 and QP980, strain hardenability was not significantly affected at high rates, confirmed by the similar percentage increase of both the ultimate tensile strength and the yield strength for the two materials (~7%).

Uniform elongation is an indication of material ductility and has a strong influence on the energy absorption capabilities of the materials, both of which are very important properties to be considered when selecting materials to be used on structural members in vehicles. As in the case of tensile strength, the phases in the microstructure affect the response of the material to changes in strain rate. Figure 4c shows the percentage change in uniform elongation for the four materials. The uniform elongation of both CR5 and SS 201 decreased at high rates, agreeing with the classic theory of strain rate sensitivity, which dictates that ductility decreases with the increase in strain rate (for materials with a positive strain rate sensitivity). DP980 showed almost no change in the uniform elongation which agrees with the insignificant strain rate sensitivity observed in terms of the yield and ultimate tensile strengths. A similar behavior would be expected of QP980, as the increase in the strength was not significant; however, its uniform elongation increased by ~21% at the higher rate. This behavior does not conform to the definition of positive nor negative strain rate sensitivity.

Energy absorbed until fracture is critical to the performance of the material during a vehicle crash incident, and this property can be represented by toughness. Though toughness depends on both strength and ductility, it is difficult to predict its change by simply looking at the changes in strength and ductility curves in Figure 4a-c; their combined effect is what matters. Figure 4d compares the effect of strain rate on the toughness of the four materials. As noted, the percentage increase of toughness for DP980 and QP980 was the highest (~28% and ~30%, respectively), followed by SS 201 which showed an increase of ~21%, and finally CR5 showed a negligible increase of only ~5%. In summary, it is clear here that the four materials (driven by their different microstructures) responded differently to increasing strain rate, leading to net change in toughness observed in Figure 4d. Total ductility reduction in CR5 at high rates counter-acted the increase in the strength, leading to a small increase in toughness. Toughness increase in SS 201 was strength-driven, since total ductility remained unchanged, while toughness increase in both DP980 and QP980 was primarily ductility-driven.

4 Discussion

All the aforementioned results suggest that the phases present in the microstructure of a steel greatly affects its response to increasing loading rates. Based on Orowan's principle [20], strain rate is directly proportional to dislocation velocity and other dislocation parameters. When materials are loaded at high rates, the density and the speed of dislocations are higher; but it is well-known that the dislocation velocity is directly related to the critical resolved shear stress [21], suggesting that higher stress is needed to overcome the critical resolved shear stress to move the dislocations at the speed required for the strain rate. This in turn implies higher yield and flow stresses during deformation at high rates, and hence reduced ductility.

The above coincides with the behavior of CR5 at high rates, where the ultimate tensile strength increased significantly; but when looking at the results of DP980, the strain rate sensitivity dropped at higher rate. To explain this, it is important to look closely at what happens during high rate testing. Under quasi-static conditions, test duration is long giving more time for heat generated during the test to be dissipated, thus a small increase in temperature is observed; it is therefore well established in the literature that isothermal conditions take place during quasi-static testing. This is not the case during high rate testing where the test occurs in a very short period of time; the 500 s^{-1} tests carried out in this study were completed within 0.4ms. In this short period of time, the generated heat doesn't have enough time to be dissipated and thus the specimen's temperature increases significantly, changing the condition from isothermal to adiabatic. For CR5 mild steel, which consists of soft and ductile ferrite only, the effect of temperature rise softening is not as significant as the work hardening due to the higher loading rate, thus the net effect

is significant increase in strength at higher rates. On the other hand, there are two opposing effects taking place in the DP980: work hardening which occurs in the ferrite; and softening due to temperature rise, which occurs primarily in the martensite, a hard and a brittle phase. The latter was reported in the work of Wang et al. 2013 [22], which showed a slight decrease in strength and an appreciable increase in ductility in a Martensitic steel as the result of increase in deformation rate. The combined effect of the aforementioned is the reduced strain rate sensitivity observed in the DP980. In regards to ductility, the net change in uniform elongation is almost zero, since the drop in ductility of ferrite is balanced by the increase in ductility in the martensite. On the other hand, the total elongation of the material increases, since the post-necking elongation portion increases (this is the case with all four steels regardless of the microstructure). Note the post-necking elongation of ~12-20% strains in all four materials at 500 s^{-1} _ significantly higher than the quasi-static post-necking strains. This is believed to be primarily driven by the localized temperature increase, shifting the necking from localized to diffused, and thus prolonging the deformation.

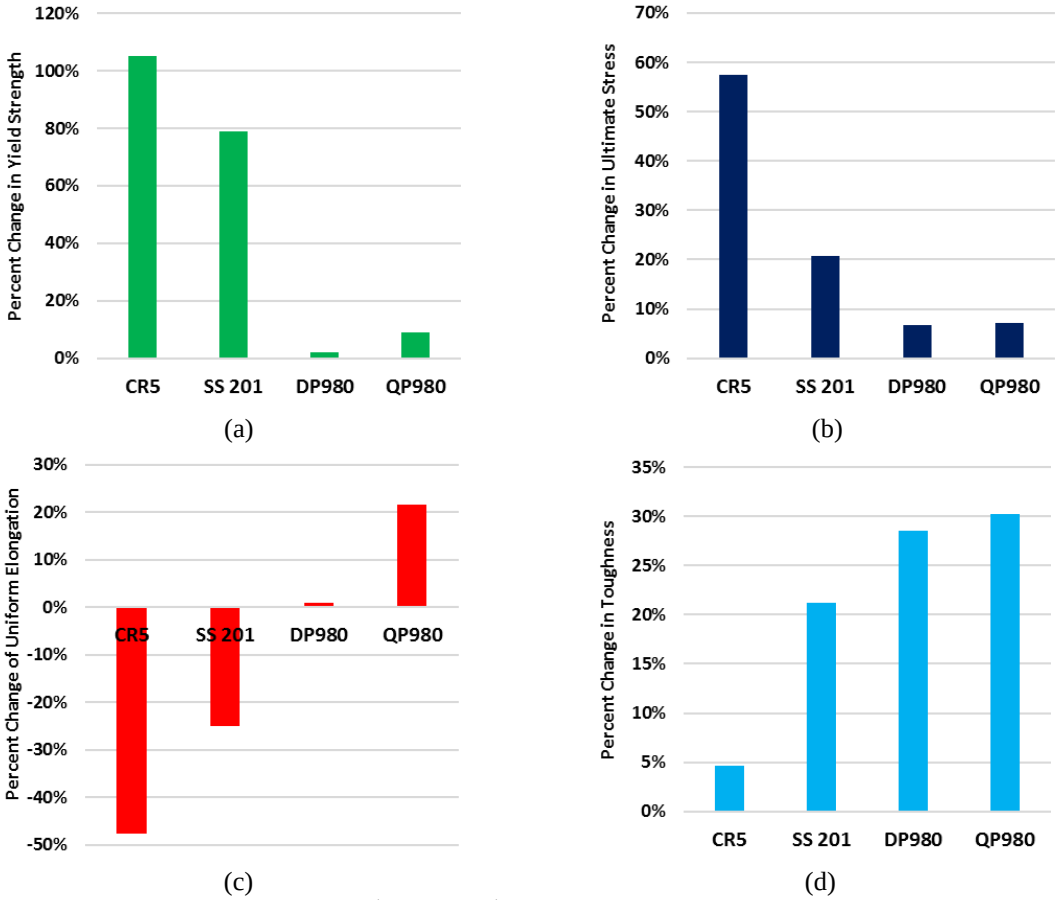

Figure 4: Percent Change between 0.005s^{-1} and 500s^{-1} of (a) Yield Stress (b) Ultimate Tensile Strength (c) Uniform Elongation and (d) Toughness.

For QP980, the small increase in strength at higher loading rate is similar to that observed in DP980, which can be attributed to the similarities in the microstructure in terms of the presence of martensite and ferrite. The slightly lower martensite and slightly higher ferrite volume fractions in QP980 (compared to DP980) results in the slightly higher rate sensitivity (Figure 4a and b). But in terms of ductility (Figure 4c), QP980 showed an increase of ~21% in uniform ductility at higher rate, which is significantly higher than that exhibited by DP980. Since this cannot be driven by the ferrite/martensite portion of the microstructure, it is believed to be associated with the austenite present in QP980. However, the effects and exact mechanisms are not clear. While austenite is known to exhibit deformation induced transformation into martensite, causing additional resistance to necking and thus enhanced tensile ductility and strain hardening, it is well established in the literature that the austenite-to-martensite transformation is inhibited at high rates since temperature increase reduces the chemistry driving force and increases the stacking fault energy, which have the combined effect of inhibiting the transformation. The results presented in Talonen et al. 2005 [23] and

Lichtenfeld et al. 2006 [24] clearly show that for several austenitic stainless steels. The results obtained in this work also support that; note the drop in uniform ductility in the SS 201 at high rates (Figure 3b and Figure 4c). So this does not really agree nor explain why QP980 exhibits improved uniform ductility, on the level of ~20%, at high rates. In fact, the effects of high loading rates on the austenite-to-martensite transformation in TRIP-assisted steels (including QP steels) is not fully understood. While some researchers claim that transformation should be inhibited at high rates (based on the results in fully austenitic stainless steels), others indicate the opposite. For instance, Liu et al. [25] showed that at strain rates higher than $100s^{-1}$, QP980 shows increased ductility (which is similar to the results shown here in Figure 3d). Liu et al. also measured the austenite content in the material after deformation and showed that the transformation is actually faster at higher rates. In summary, there are some uncertainties in this area that require further investigation to help understand the transformation kinetics dependence on strain rate (in austenite), and thereafter the impacts of this on the response of TRIP-assisted steels (such as the QP980).

5 Summary and Conclusions

The effects of the phase content on the strain rate sensitivity in two ~1GPa tensile strength steels, Ferrite-Martensite DP980 and Ferrite-Martensite-Austenite QP980, were investigated. Ferritic CR5 mild steel and austenitic stainless steel 201 were also studied for comparison. The materials were deformed at 0.005 and 500 s^{-1}, and their mechanical response was examined. DP980 showed almost no rate sensitivity; slight increase in strength and drop in uniform ductility at higher deformation rate. This was attributed to the opposite effects of ferrite and martensite balancing out. Ferrite is known to have a positive strain rate sensitivity, which was confirmed by the results obtained here for CR5. Martensite is known to have a negative strain rate sensitivity that is primarily driven by high temperature softening at higher rates. QP980 was also shown to exhibit negligible rate sensitivity in regards to strength; however, QP980 showed notable enhanced uniform ductility, which cannot be explained based on the known responses of the individual phases. Even austenite, the highly ductile phase, is known to exhibit a drop in uniform ductility at high rates due to the inhibition of austenite-to-martensite transformation, which was also confirmed by the results obtained here for the SS 201. Further investigation of austenite-to-martensite transformation kinetics and its rate dependence is ongoing to help explain the response of TRIP-assisted steels (such as QP980) at higher rates. Toughness in both DP980 and QP980 was shown to improve significantly at rates close to crash conditions, which compared favorably to the conventional CR5 mild steel that showed no increase in toughness. It is important to note here that the differences in behaviors of these steels are not merely driven by their microstructures and phases contents; other parameters like chemical composition play important roles. The ferrite in CR5, for instance, is not exactly the same as the ferrite in DP980 or QP980. The comparisons made in this study on the basis of phases were done to extract general trends to help explain the responses of steels with two or more phases in their microstructures.

Acknowledgements

The authors greatly acknowledge the support of the Department of Energy, for funding this work. The support of General Motors, ThyssenKrupp Steel and AK Steel for supplying the materials used in this work is also acknowledged.

This material is based upon work supported by the Department of Energy under Cooperative Agreement Number DE-EE0005976, with United States Automotive Materials Partnership LLC (USAMP). This report was prepared as an account of work sponsored by an agency of the United States Government. Neither the United States Government nor any agency thereof, nor any of their employees, makes any warranty, express or implied, or assumes any legal liability or responsibility for the accuracy, completeness, or usefulness of any information, apparatus, product, or process disclosed, or represents that its use would not infringe privately owned rights. Reference herein to any specific commercial product, process, or service by trade name, trademark, manufacturer, or otherwise does not necessarily constitute or imply its endorsement, recommendation, or favoring by the United States Government or any agency thereof. The views and opinions of authors expressed herein do not necessarily state or reflect those of the United States Government or any agency thereof.

References

[1] Keeler, Stuart, and Menachem Kimchi. Advanced High-Strength Steels Application Guidelines V5. WorldAutoSteel, 2015.

[2] Curtze, S., Kuokkala, V. T., Hokka, M., & Peura, P. (2009). Deformation behavior of TRIP and DP steels in tension at different temperatures over a wide range of strain rates. Materials Science and Engineering: A, 507(1), 124-131.

[3] Tarigopula, V., Hopperstad, O. S., Langseth, M., Clausen, A. H., & Hild, F. (2008). A study of localisation in dual-phase high-strength steels under dynamic loading using digital image correlation and FE analysis. International Journal of Solids and Structures, 45(2), 601-619.
[4] Huh, H., Kim, S. B., Song, J. H., & Lim, J. H. (2008). Dynamic tensile characteristics of TRIP-type and DP-type steel sheets for an auto-body. International Journal of Mechanical Sciences, 50(5), 918-931.
[5] Huh, H., Lim, J. H., & Park, S. H. (2009). High speed tensile test of steel sheets for the stress-strain curve at the intermediate strain rate. International Journal of Automotive Technology, 10(2), 195-204.
[6] Curtze, S., Kuokkala, V. T., Hokka, M., & Peura, P. (2009). Deformation behavior of TRIP and DP steels in tension at different temperatures over a wide range of strain rates. Materials Science and Engineering: A, 507(1), 124-131.
[7] Huh, H., Lee, H. J., & Song, J. H. (2012). Dynamic hardening equation of the auto-body steel sheet with the variation of temperature. International Journal of Automotive Technology, 13(1), 43-60.
[8] Xu, S., Ruan, D., Beynon, J. H., & Rong, Y. (2013). Dynamic tensile behaviour of TWIP steel under intermediate strain rate loading. Materials Science and Engineering: A, 573, 132-140.
[9] Kim, J. H., Kim, D., Han, H. N., Barlat, F., & Lee, M. G. (2013). Strain rate dependent tensile behavior of advanced high strength steels: Experiment and constitutive modeling. Materials Science and Engineering: A, 559, 222-231.
[10] Qin, J., Chen, R., Wen, X., Lin, Y., Liang, M., & Lu, F. (2013). Mechanical behaviour of dual-phase high-strength steel under high strain rate tensile loading. Materials Science and Engineering: A, 586, 62-70.
[11] Huh, J., Huh, H., & Lee, C. S. (2013). Effect of strain rate on plastic anisotropy of advanced high strength steel sheets. International Journal of Plasticity, 44, 23-46.
[12] Danyang, D. O. N. G., Yang, L. I. U., Lei, W. A. N. G., & Liangjin, S. U. (2013). Effect of strain rate on dynamic deformation behavior of DP780 steel. Acta Metall Sin, 49(2), 159-166.
[13] Yang, X., Hector Jr, L. G., & Wang, J. (2014). A combined theoretical/experimental approach for reducing ringing artifacts in low dynamic testing with servo-hydraulic load frames. Experimental Mechanics, 54(5), 775-789.
[14] Li, S., Kang, Y., Zhu, G., & Kuang, S. (2015). Effects of strain rates on mechanical properties and fracture mechanism of DP780 dual phase steel. Journal of Materials Engineering and Performance, 24(6), 2426-2434.
[15] Hwang, B. C., Cao, T. Y., Shin, S. Y., Kim, S. H., Lee, S. H., & Kim, S. J. (2005). Effects of ferrite grain size and martensite volume fraction on dynamic deformation behaviour of 0· 15C–2· 0Mn–0· 2Si dual phase steels. Materials science and technology, 21(8), 967-975.
[16] Oliver, S., Jones, T. B., & Fourlaris, G. (2007). Dual phase versus TRIP strip steels: Microstructural changes as a consequence of quasi-static and dynamic tensile testing. Materials characterization, 58(4), 390-400.
[17] Li, S., Zou, D., Xia, C., & He, J. (2015). Effect of strain rate on deformation-induced martensitic transformation of quenching and partitioning steels. steel research international.
[18] Mates, S., Abu-Farha, F. (2015). Dynamic tensile behavior of a quenched and partitioned high strength steel using a kolsky bar. Proceedings of the 2015 SEM Annual Conference and Exhibition (SEM 2015), Costa Mesa, CA, 08th - 11th June 2015.
[19] Verleysen, P., Peirs, J., Van Slycken, J., Faes, K., & Duchene, L. (2011). Effect of strain rate on the forming behaviour of sheet metals. Journal of Materials Processing Technology, 211(8), 1457-1464.
[20] Qin, K., Yang, L. M., & Hu, S. S. (2014). Interpretation of strain rate effect of metals. In Dynamic Behavior of Materials, Volume 1 (pp. 21-27). Springer International Publishing.
[21] Gilman, J. J., & Johnston, W. G. (1957). Dislocations and mechanical properties of crystals. Fisher, J., Johnston, W., Thomson, R., Vreeland, T.(eds.), 116.
[22] Wang, W., Li, M., He, C., Wei, X., Wang, D., & Du, H. (2013). Experimental study on high strain rate behavior of high strength 600–1000MPa dual phase steels and 1200MPa fully martensitic steels. Materials & Design, (47), 510-521.
[23] Lichtenfeld, J. A., Van Tyne, C. J., & Mataya, M. C. (2006). Effect of strain rate on stress-strain behavior of alloy 309 and 304L austenitic stainless steel. Metallurgical and Materials Transactions A, 37(1), 147-161.
[24] Talonen, J., Hänninen, H., Nenonen, P., & Pape, G. (2005). Effect of strain rate on the strain-induced $\gamma \rightarrow \alpha'$-martensite transformation and mechanical properties of austenitic stainless steels. Metallurgical and materials transactions A, 36(2), 421-432.
[25] Liu, C., Wang, L., & Liu, Y. (2013, March). Effects of strain Rate on tensile deformation behavior of quenching and partitioning steel. In Materials Science Forum (749), 401-406.